Article

Theoretical Study of Binding of Metal-Doped Graphene Sheet and Carbon Nanotubes with Dioxin

Hong Seok Kang

J. Am. Chem. Soc., **2005**, 127 (27), 9839-9843• DOI: 10.1021/ja0509681 • Publication Date (Web): 17 June 2005

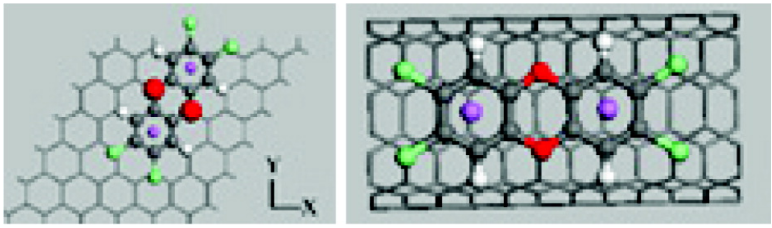

Journal of the American Chemical Society is published by the American Chemical Society. 1155 Sixteenth Street N.W., Washington, DC 20036

J|A|C|S
ARTICLES
Published on Web 06/17/2005

Theoretical Study of Binding of Metal-Doped Graphene Sheet and Carbon Nanotubes with Dioxin

Hong Seok Kang*

Contribution from the College of Natural Science, Jeonju University, Hyoja-dong, Wansan-ku, Chonju, Chonbuk 560-759, Republic of Korea

Received February 15, 2005; E-mail: hsk@jj.ac.kr

Abstract: Using density functional theory, we have theoretically studied dioxin binding on a graphene sheet or carbon nanotubes (CNT), finding that they can be effective adsorbents for dioxin in the presence of calcium atoms. This is due to a cooperative formation of sandwich complexes of graphene sheet or (5,5) CNT through the interaction π−Ca−π with the total binding energy of more than 3 eV. This correlates with the band structure analysis, which indicates charge transfer from the carbon systems and calcium atoms to dioxin when the molecule binds to the metal-doped carbon systems. For CNT with small radii, the relative strength of CNT−dioxin interaction is dependent on their chiralities. Upon dioxin binding, a large increase in the electronic density of states near the Fermi level also suggests that they can be used for dioxin sensing. Fe-doped CNT is also found to bind dioxin strongly, revealing an important role played by remnants of metallic catalysts in the chemical properties of CNT.

1. Introduction

Dioxins (Dx) are known to be highly toxic as a cancer hazard. In addition, they cause severe developmental problems, damage the immune system, and interfere with hormonal systems.[1] Their chemical stability and widespread presence require a highly efficient method to remove them to well below 1 ng/m^3. Recently, carbon nanotubes (CNT) were shown to be an even more efficient sorbent than the activated carbon widely used for dioxin removal.[2] For this method, it is not clear if the observed binding to the CNT is entirely due to the direct adsorption of the molecule on the CNT or if some other kinds of mechanisms are involved. Related to this, it would be interesting to investigate how strong the binding of dioxin on the CNT is when the adsorption is mediated by metallic atoms M. This is particularly so, since the π−metal−π interaction is generally much stronger than the direct π−π interaction.

Also, it will be interesting to investigate the possibility of using graphite for dioxin removal, since it is available in much larger amounts as well as much cheaper than the CNT. However, the extreme toxicity of dioxin limits the experimental investigation of these problems. An alternative is a theoretical calculation based on a highly reliable and efficient method. For this, we recall that density functional theory (DFT) explained later in the article was shown to describe an interaction in the benzene−M−benzene sandwich complex very successfully, being almost as reliable as the much more sophisticated method G3(MP2).[3] Since dioxin-sensing of the present day mostly relies on a time-consuming process involving condensation and purification, it is also desirable to devise a more efficient way of sensing it that would function by using a simple mechanism in a ubiquitous situation. It would be interesting to investigate if carbon nanotubes can be used for such a purpose, noting that carbon nanotubes and nanowires have been widely proposed for sensing gas molecules.[4]

This work is focused on the theoretical understanding of the binding of dioxin in Gr−M−Dx and CNT−M−Dx sandwich complexes, where Gr is a graphene sheet and M is either lithium or calcium. In the first-order approximation, the graphene sheet represents a graphite surface, since the interaction of the surface with inner graphitic planes is weak.[5] In addition, it also represents a CNT with a very large diameter, since a CNT is simply generated by rolling up the sheet. Lithium-doping to the graphite or the CNT has been widely studied both theoretically and experimentally.[6] Calcium is of interest in respect to its ability to lose two electrons and the role of its empty d-orbitals.[7] Since metallic catalysts can remain doped on the CNT even

---

(1) Hileman, B. *Chem. Eng. News* **2000**, *29*, 13.
(2) Long, R. Q.; Yang, R. T. *J. Am. Chem. Soc.* **2001**, *123*, 2058.
(3) Kang, H. S. *J. Phys. Chem. A* **2005**, *109*, 478.
(4) (a) Kong, J.; Franklin, N. R.; Zhou, C.; Chapline, M. G.; Peng, S.; Cho, K.; Dai, H. *Science* **2000**, *287*, 622. (b) Favier, F.; Walter, E. C.; Zach, M. P.; Benter, T.; Penner, R. M. *Science* **2001**, *293*, 2227. (c) Qi, P.; Vermesh, O.; Grecu, M.; Javey, A.; Wang, Q.; Dai, H.; Peng, S.; Cho, K. J. *Nano Lett.* **2003**, *3*, 347. (d) Peng, S.; Cho, K. *Nano Lett.* **2003**, *3*, 513. (e) Besteman, K.; Lee, J.-O.; Wiertz, F. G. M.; Heering, H. A.; Dekker, C. *Nano Lett.* **2003**, *3*, 727. (f) da Silva, L. B.; Fagan, S. B.; Mota, R. *Nano Lett.* **2004**, *4*, 65. (g) Liu, H.; Kameoka, J.; Czaplewski, D. A.; Craighead, H. G. *Nano Lett.* **2004**, *4*, 671. (h) Ramanathan, K.; Bangar, M. A.; Yun, M.; Chen, W.; Mulchandani, A.; Myung, N. V. *Nano Lett.* **2004**, *4*, 1237. (i) Bekyarova, E.; Davis, M.; Burch, T.; Itkis, M. E.; Zhao, B.; Sunshine, S.; Haddon, R. C. *J. Phys. Chem. B* **2004**, *108*, 19717.
(5) Even the electronic structure of a bulk graphite is only weakly perturbed from that of a graphene sheet up to a high energy (= 9 eV) above Fermi level. For this, see Charlier, J.-C.; Gonze, X.; Michenaud, J.-P. *Phys. Rev. B* **1991**, *43*, 4579.
(6) (a) Winter, M.; Besenhard, J. O.; Spahr, M. E.; Novak, P. *Adv. Mater.* **1998**, *10*, 7259. (b) Gao, B.; Kleinhammes, A.; Tang, X. P.; Bower, C.; Fleming, L.; Wu, Y.; Zhou, O. *Chem. Phys. Lett.* **1999**, *307*, 153. (c) Zhao, J.; Buldum, A.; Han, J.; Lu, J. P. *Phys. Rev. Lett.* **2000**, *85*, 1706. (d) Dubot, P.; Cenedese, P. *Phys. Rev. B* **2001**, *63*, 241402R.
(7) Kang, H. S. *J. Phys. Chem. A* **2005**, *109*, 1458.

10.1021/ja0509681 CCC: $30.25 © 2005 American Chemical Society

after the accomplishment of the CNT synthesis, we also consider the system CNT−Fe−Dx to understand the role of the remnants in dioxin binding.

2. Theoretical Methods

Our total energy calculations are based on the solution of the Kohn−Sham (KS) equation within the generalized gradient approximation due to Perdew, Berke, and Ernzerhof.[8] Calculations are done on an IBM-SP3 parallel supercomputer with the Vienna ab initio Simulation Program,[9] using the projected augmented wave method[10] with a cutoff energy of 400 eV. For structure optimization, atoms are relaxed to the direction of the Hellmann−Feynman force using the conjugate gradient method, until a stringent convergence criteria (= 0.03 eV/Å) is satisfied. The valence electron as well as the 1s^2 electrons of a Li atom are explicitly treated in the KS equation. Similarly, all the valence electrons and 3p^6 electrons are considered in the equation for Ca and Fe. Graphite is modeled by a graphene sheet in a periodic supercell, which consists of 6 × 6 primitive cells of a two-dimensional hexagonal lattice. Calculations with various lattice parameters show that the optimal parameter is 14.62 Å. For this, energy minimizations are performed at various lattice constants to calculate total energy as a function of the lattice constant. When a Dx molecule sits on the Gr, the shortest distance between non-hydrogen atoms of dioxins in the neighboring cells is 4.46 Å. The total number of atoms considered is 84∼92, depending upon the system. Our calculation shows that the effect of artificial interaction between dioxin molecules in the neighboring cells is less than 0.02 eV in the most extreme case.[11] A large distance (= 12.0 Å) is maintained along the direction perpendicular to the plane of the sheet. For CNT, we consider (5,5) armchair CNT with 120 atoms in a supercell of the dimension of 14.85 Å along the tube axis. This results in the closest distance of 4.73 Å between chlorine atoms of dioxin molecules in the neighboring cells when a dioxin molecule sits on the tube. A large distance is also maintained along the directions perpendicular to the tube axis. For the graphene systems, *k*-space sampling is done with three points including the Γ-point in the irreducible region of the Brillouin zone, while two *k*-points are used for the CNT systems along the direction of the tube axis. Therefore, taking into account the number of atoms and the number of *k*-points described above, the present work requires a heavy computation even on a massively parallel supercomputer. As a typical dioxin, we consider 2,3,7,8-tetrachlorodibenzo-*p*-dioxin or TCDD. It consists of three six-membered rings that are aligned parallel to each other in a coplanar geometry.

3. Results

We first consider the binding processes Gr + 2M → Gr−2M (“P1”) and Gr−2M + Dx → Gr−2M−Dx (“P2”) for M = Li or Ca. For process P1, we consider two metal atoms M on the opposite sides of the graphene sheet, that is, one on top of the center of a hexagon of the graphene sheet, and the other on the bottom of the center of another hexagon far from the first one. (We recall that it is well-known that a Li atom binds to the carbon nanotube on top of a hexagon.) This will evidently minimize charge−charge interaction between two metal atoms when they are positively charged. Table 1 shows that the binding energies [=E_b(P1, Li) and E_b(P1, Ca)] of this process for M = Li and Ca are −2.10 and −0.89 eV, respectively. Ca atoms exhibit much weaker binding to the graphene sheet than Li atoms. M−Gr distances are 1.74 and 2.36 Å for M = Li and Ca, respectively. In process P2, we assume that M atoms rearrange themselves so that Gr−2M−Dx form a sandwich complex, where two M atoms are now located between the planes of Gr and Dx. Figure 1 shows the system viewed along an axis (= *Z* axis), which is perpendicular to those planes. The Dx molecule was assumed to lie on the Gr in such a way that carbon atoms of the Dx are located directly above those of the Gr. For this, we note that a similar configuration has been proposed for sandwich complexes of benzene−Li−benzene.[3] We find that the binding energies E_b(P2, M) are −1.05 and −2.31 eV for M = Li and Ca, respectively. We have already noted that Gr−Ca binding is much weaker than that of Gr−Li in the absence of Dx. However, there is a strong cooperative binding among Gr−2Ca−Dx.

Table 1. Binding Energy in Electronvolts of the Process Defined in the First Column for the Sandwich Complexes Gr−2M−Dx, CNT−2M−Dx, and Dx−2M−Dx, Where Gr, CNT, and Dx Denote the Graphene Sheet, (5,5) CNT, and a Dioxin Molecule[a]

M	Li			Ca			Fe
X	Gr	CNT	Dx	Gr	CNT	Dx	CNT
2M + X → 2M−X	−2.10	−2.76	−0.48	−0.89	−1.51	−0.50	−2.02
2M−X + Dx → X−2M−Dx	−1.05	−0.58	−1.32	−2.31	−2.05	−1.98	−3.49
2M + X + Dx → X−2M−Dx	−3.15	−3.34	−1.80	−3.20	−3.56	−2.48	−5.51

[a] M is Li or Ca. CNT−2Fe−Dx is also considered.

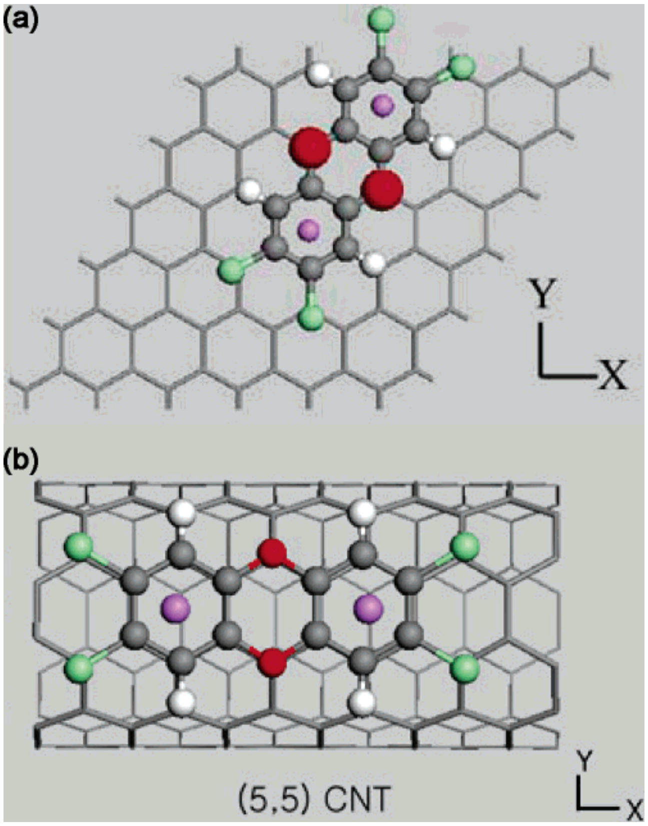

Figure 1. (a) Dioxin molecule on the surface of 6 × 6 primitive cells of the graphene sheet in the complex Gr−2M−Dx. For clarity, oxygen atoms are shown with large spheres. (b) Dioxin molecule on the surface of (5,5) CNT. Metal atoms are shown at the center of two hexagons. Coordinate system is also defined.

---

(8) Perdew, J. P.; Burke, K.; Ernzerhof, M. *Phys. Rev. Lett.* **1996**, *77*, 3865.
(9) Kresse, G.; Hafner, J. *Phys. Rev. B* **1993**, *47*, RC558.
(10) Kresse, G.; Furthmuller, J. *Phys. Rev. B* **1996**, *54*, 11169.
(11) The maximum interaction energy (= 0.02 eV) between dioxin molecules of neighboring cells was estimated from the analysis of the Dx−Ca−Dx system, since it is also subject to charge transfer from Ca to Dx molecules as in the case of the system Gr−Ca−Dx. For comparison, the total energy of a dioxin molecule in a much larger supercell was considered as a reference. For better understanding, it is recommended that readers reconsider this problem after reading the next section.

In the optimized structure of Gr−2Li−Dx, there is practically no deformation in the geometry of Gr and Dx (i.e., they remain planar). Li is located almost in the middle of the two planes of Dx and Gr. Distances of Gr−Li and Dx−Li (= 1.93 and 1.95 Å) are larger than that (= 1.74 Å) of Gr−Li in the complex of Gr−2Li without Dx. On the other hand, the geometry of the Ca complex is characterized by a deformation of Dx in such a way that oxygen atoms protrude from the planes of the aromatic rings of Dx by approximately 0.12 Å so that it gets away from the plane of Gr. Chlorine atoms also slightly deviate from the plane of the molecule so that the molecule would adopt a twisted conformation with C_2 symmetry. The Gr adopts a slightly bowl-shaped conformation, and the Ca atoms sit on its concave side. Gr−Ca and Dx−Ca distances (= 2.35 and 2.45 Å) are comparable to that (= 2.36 Å) of Gr−Ca in the complex Gr−2Ca.

From the geometry of dioxin and the observations given above, we can easily expect that CNT−dioxin interaction would be different for CNTs of different chiralities. For armchair CNTs, the dioxin molecule would align on the tube parallel to the tube axis so that the dioxin molecule adopts an “in-phase” orientation (i.e., three rings of the dioxin molecule sit directly on top of three rings of the CNTs along the tube axis; see Figure 1b). In those CNTs, all of the six-membered rings of the CNT adjacent to each other along the tube axis lie on a single plane, which is not the case in other chiralities. In zigzag CNTs, the in-phase orientation is achieved when the dioxin molecule sits on the CNT along the direction of circumference. In this orientation, the curvature of the CNT along that direction would not allow a strong interaction among CNT−2M−Dx, unless there are deformations in the geometries of both the CNT and the dioxin molecule. This will be the case particularly for the CNTs with small radii. For example, our calculation shows that (10,0) CNT undergoes a flattening of the sidewall on the side involved in the sandwich formation. Despite its diameter being larger by 15%, the binding strength for the overall process CNT + 2M + Dx → CNT−2M−Dx (process “C1 + C2”) is weaker than that of the (5,5) CNT shown in Table 1 by 0.55 eV. Such a deformation will be more difficult for the CNTs with smaller radii, leading to still weaker binding in the sandwich complex. In short, armchair CNTs are the best for the interaction of our interest, and we will concentrate on (5,5) CNT hereafter. Table 1 shows the binding energies for CNT−2M−Dx defined similarly to the case of Gr−2M−Dx. In the complexes CNT−2M, to be more stringent, we assume that two metal atoms are on the opposite sides of the circumference of the CNT. The table shows that the binding of dioxin on the complex CNT−2Li is apparently much less favorable than the corresponding binding on the complex Gr−2Li, while the complex CNT−2Ca is almost as effective as Gr−2Ca. Little deformation is observed in the planar geometry of the dioxin molecule for the CNT−2Li−Dx, while appreciable deformation is observed for the calcium sandwich complex, resulting in a twisted conformation of dioxin. In both lithium and calcium sandwich complexes, M−CNT and M−Dx distances are almost the same as their correspondents in the complex Gr−2M−Dx.

To investigate the possible role of the remnants of the catalysis used for CNT synthesis on the binding of dioxin, we have made a time-consuming calculation for the binding energy of dioxin on the surface of the (5,5) CNT when the CNT is doped with iron atoms. In Table 1, our spin-polarized calculation shows that Fe-doped CNT also can be a good sorbent for dioxin. It is very interesting to note that the binding energy (= −3.49 eV) of the process CNT−2Fe + Dx → CNT−2Fe−Dx corresponds to Long and Yang’s binding energy of dioxin on the CNT surface. In addition, our separate calculation shows that there is also practically no direct binding of Dx on the CNT. This seems to be consistent with a recent MP2 calculation on a benzene−benzene dimer using a very large basis set, which has shown that the direct benzene−benzene interaction is less than −0.12 eV.[12] Therefore, Fe-doping to CNT is a much more efficient way of adsorbing dioxin than direct adsorption.

For comparison, we have also considered the processes 2M + Dx → 2M−Dx (process “H1”) and 2M−Dx + Dx → Dx−2M−Dx (process “H2”). In the former process, as in the case of Gr−2M or CNT−2M, one of the two atoms of M is assumed to bind to the top of the center of an aromatic ring, and the other atom to the bottom of the center of another aromatic ring in the dioxin molecule. Therefore, we are also assuming that one of the two M atoms moves to the region between the two dioxin planes in process H2. Table 1 shows that E_b(H1,M) = −0.48 and −0.50 eV for M = Li and Ca, respectively. E_b(H2,M) is found to be −1.32 and −1.98 eV. In short, there are also cooperative bindings among Dx−2M−Dx. However, when dioxin molecules are added to the complex of 2M−Gr, the comparison of the binding energy data for overall processes in Table 1 shows that resulting products will be dominated by a heterocomplex Gr−2M−Dx rather than the homocomplex Dx−2M−Dx on a purely energetic ground. Since dioxin molecules usually exist in ppm units in pollutants, there is even a much smaller chance of forming the homocomplex if Gr and M exist in much larger concentrations. Effectively, all of the dioxin molecules will be involved in the formation of the complex Gr−2M−Dx. In short, process H2 can be effectively ignored. This implies that the Gr−M complex can be a very efficient system for capturing dioxin molecules. The Gr−2Ca system can be especially efficient for this purpose in view of the large cooperativity in the formation of the complex among three species when a pollutant, including dioxin molecules, passes through it.

To have better insight into the nature of the binding in these complexes, Figure 2 shows the band structures of the systems Gr−2M−Dx in comparison with that of a pure graphene sheet. All of the bands of the latter shown in the figure correspond to π-bands. Twofold degeneracy at point K for the primitive cell folds back to the Γ-point in the case of our supercell with 6 × 6 primitive cells. The complex formation introduces a splitting of doubly degenerate bands of the original graphene sheet. For M = Li, we first find that there is a flat band at −2.77 eV below the Fermi level, representing HOMO of the dioxin molecule. On one hand, the LUMO of dioxin is located at approximately +0.24 eV. In addition, two conduction bands (= LUMO and LUMO+1) of the original graphene sheet get half-filled, as can be seen from the shift of the Fermi level. This implies that the interaction among the three species can be described as an electrostatic one in $Gr^{-2}-2Li^{+}-Dx$. A strong electrostatic interaction is expected between the graphene sheet and Li after the charge transfer from the lithium atoms to the

---

(12) Sinnokrot, M. O.; Valeev, E. F.; Sherrill, C. D. *J. Am. Chem. Soc.* **2002**, *124*, 10887.

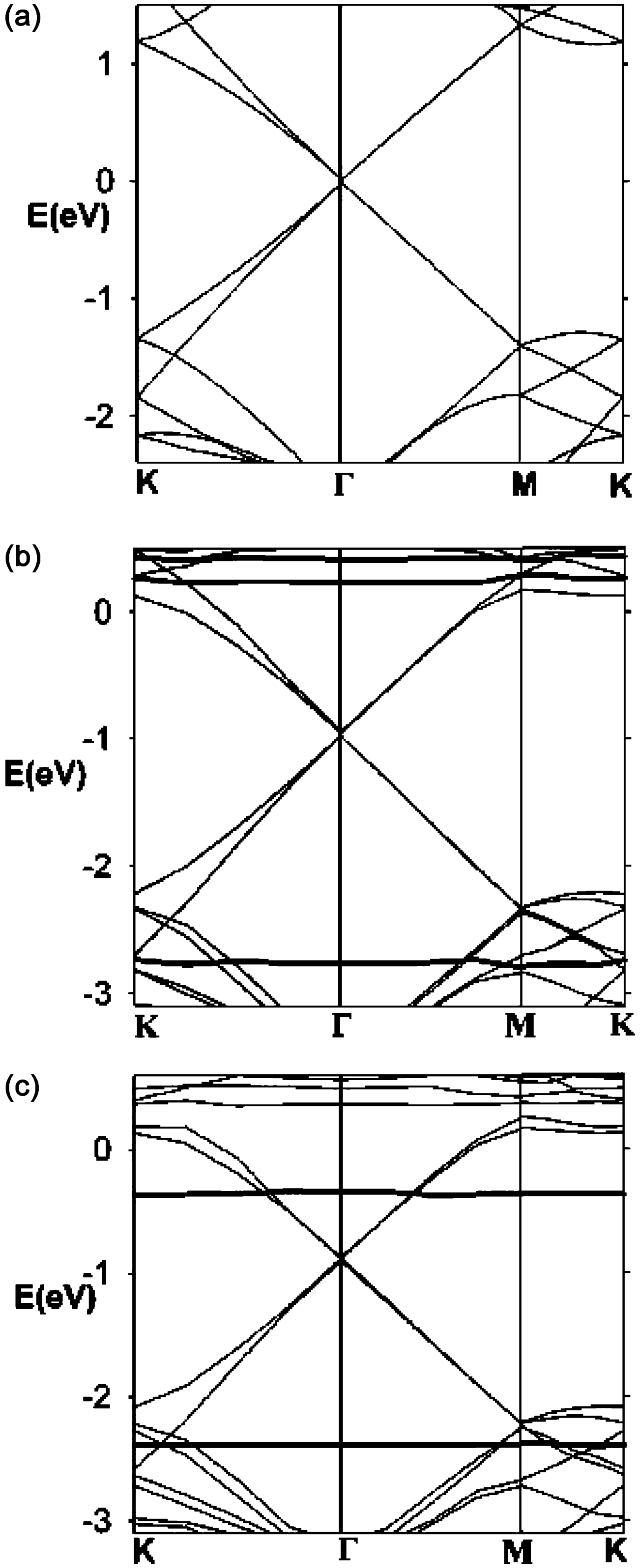

Figure 2. Band structures of a pure graphene sheet of 6 × 6 primitive cells (a) and the complexes Gr+2Li+Dx (b) and Gr+2Ca+Dx (c). In each case, the Fermi level is separately defined as energy zero. The nearly flat bands, represented by thick lines, are derived from molecular states of dioxin.

Gr. On the other hand, the dioxin molecule is expected to gain little charge, and there is a relatively weak cation−π interaction between Li and dioxin. This explains the relative weakness of the binding ($E_b = -1.05$ eV) for process P2 compared to that (= −2.10 eV) for process P1. For this, we have also made a band structure calculation for the complex Gr−2Li (not shown here), which indicates that LUMO and LUMO+1 of the original graphene sheet become also half-filled in this complex. This indicates that there is already a charge transfer in this complex, resulting in 2Li^{+}−Gr^{-2}. The addition of a dioxin molecule to this system merely introduces cation−π interaction.

Figure 2c also shows the band structure of the system Gr+2Ca+Dx. In this case, we find two flat bands below the Fermi level. One is the HOMO of the dioxin molecule lying at −2.38 eV, and the other band at −0.37 eV is its LUMO interacting with the 3d$_{xy}$ state of calcium atoms. As in the case of Li complex, the LUMO and LUMO+1 bands of the original graphene sheet get half-filled. This suggests that there is a large charge transfer from two calcium atoms to the graphene sheet and the dioxin molecule, and the charge distribution there can be simply described by Gr$^{-2+\delta}$−2Ca$^{2-\delta}$−Dx$^{-2+\delta}$, where δ is a small quantity. This is different from the case of the Li complex, in that dioxin now gains nearly two excess electrons. To investigate the reason the binding among these three species is much more cooperative than that in the case of Gr−2Li−Dx, we have also examined the band structure of the complex 2Ca−Gr (not shown). We observe two flat bands very close to the Fermi level, that is, at approximately +0.02 eV, which are 4s bands of calcium atoms. These are at most partially filled at room temperature in the Fermi−Dirac distribution. Therefore, upon the binding of calcium atoms to the graphene sheet, we expect a large charge transfer from calcium to Gr. In short, the charge distribution in Gr−2Ca is expected to be 2Ca$^{2-\delta'}$−Gr$^{-4+2\delta'}$, where δ' is a quantity larger than δ. The accumulation of more than two excess electrons solely on the graphene sheet does not seem to be energetically favorable enough, as evidenced by the relatively small binding energy E_b(P1, Ca) (= −0.89 eV) compared to E_b(P1,Li). Note that the electrostatic repulsion between two Ca atoms is negligible, because they are assumed to be separated far apart from each other (= 9.63 Å), located on the opposite sides of the graphene sheet in our model for Gr−2Ca. Therefore, when a dioxin molecule binds to this complex, Gr−2Ca, we expect that some of the excess electrons on the graphene sheet, as well as the electrons in partially occupied 4s(Ca) bands, are transferred to the low-lying LUMO band of the dioxin molecule, and this seems to be the origin of the cooperativity in the binding among Gr−2Ca−Dx. Analysis of the electronic density of states (DOS) for the complex Gr−2Ca−Dx shows that bands within 2 eV above the Fermi level are characterized by a strong interaction of the d-states of calcium atoms with π-states of the graphene sheet or π-states of dioxin, which is also responsible for a big enhancement in the DOS at the Fermi level when compared to the case of the pure graphene sheet.

Band structure calculation shows that the nature of binding in the complexes CNT−2M−DX is similar. Figure 3 shows the band structures of the complexes (5,5) CNT−2M−Dx in comparison with that of the (5,5) CNT. For both metallic complexes, we note that there is a shift of the Fermi level toward a higher energy by ∼0.4 eV. Counting the number of k-points in CNT-derived states (represented by thick solid lines in Figure 3) between the Fermi level of the pristine CNT and those of each of the metallic complexes, we find that the CNT gains approximately two more electrons upon the sandwich formation.

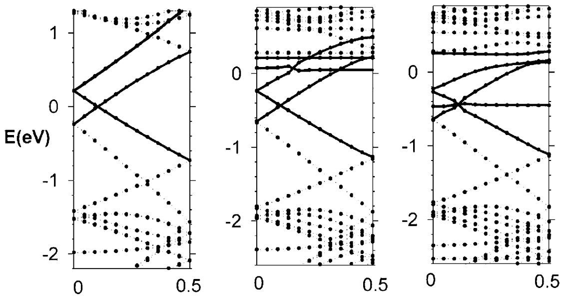

Figure 3. Band structures of (5,5) CNT, which consists of 120 atoms and its complexes: CNT (a), CNT+2Li+Dx (b), and CNT+2Ca+Dx (c). In each case, the Fermi level is separately defined as energy zero. Note that the Fermi levels of the latter two are shifted upward by approximately 0.4 eV with respect to that of the CNT. Three bands of the CNT around the Fermi level and their equivalents are represented by thick lines. The nearly flat bands, also represented by thick lines in (b) and (c), are derived from the molecular states of dioxin.

In the lithium complex, we also find two flat bands at 0.05 and 0.21 eV above the Fermi level, corresponding to LUMO and LUMO+1 of the dioxin molecule. This observation also suggests the charge distribution of $\mathrm{CNT}^{-2+\delta}-2\mathrm{Li}^{+1}-\mathrm{Dx}^{-\delta}$. Again, our separate band structure calculation on the complex CNT−2Li indicates that 2s(Li) bands appear far above the Fermi level, implying the charge distribution of $\mathrm{CNT}^{-2}-2\mathrm{Li}^{+1}$. Therefore, similar to the case of its graphite analogue, the binding of dioxin on this complex mostly introduces cation−π interaction. In the calcium complex, we find the LUMO of dioxin at −0.46 eV. Another flat band at +0.25 eV represents the LUMO+2 of dioxin. A relatively large flattening of the CNT band just below this one reflects the interaction of the CNT state with the LUMO+2 band of dioxin. In short, we expect a charge distribution of $\mathrm{CNT}^{-2+\delta}-2\mathrm{Ca}^{2-\delta}-\mathrm{Dx}^{-2+\delta}$. Similar to the case of the complex Gr−2Ca, our separate calculation on the band structure of the complex CNT−2Ca indicates that 4s(Ca)-derived states also appear very close to the Fermi level, indicating a charge distribution of $2\mathrm{Ca}^{2-\delta'}-\mathrm{CNT}^{-4+2\delta'}$. Therefore, we also expect a charge transfer from both of the CNT and calcium atoms to dioxin when a dioxin molecule binds to the complex CNT−2Ca, again contributing to the large cooperativity in the sandwich formation.

4. Conclusion

In summary, we have shown that the doping of a graphene sheet or CNTs of large diameters with calcium atoms can introduce a strong cooperative binding of carbon systems with dioxin. This suggests that a graphite surface, which is much cheaper than CNT, can be at least as efficient as CNT for dioxin removal and thus might be able to be used in incineration plants. Band structure analysis suggests that the charge transfer model can explain these observations. Iron atoms, which are commonly used as a catalyst for CNT synthesis, can also significantly facilitate dioxin binding. In a sense, this suggests that the adsorption of small molecules, particularly with delocalized π electrons, can be significantly enhanced by the presence of metallic catalyst remnants after the accomplishment of the CNT synthesis. Upon dioxin adsorption, a large increase in the electronic density of state near the Fermi level may find its application to dioxin sensing through its conductivity change. In addition, dioxin binding on CNT is chirality-dependent for the CNTs with small radii, which may be applied to the separation of CNTs according to their chiralities.

Acknowledgment. We appreciate Jeonju University for its financial support.

JA0509681